Femtosecond transition state dynamics of *cis*-stilbene

T. Baumert[1], **T. Frohnmeyer**[1], **B. Kiefer**[2], **P. Niklaus**[2], **M. Strehle**[2], **G. Gerber**[2,*], **A.H. Zewail**[3]

[1] Fachbereich Physik, Universität Kassel, 34132 Kassel, Germany
[2] Physikalisches Institut, Universität Würzburg, Am Hubland, 97074 Würzburg, Germany
(Fax: +49-931/8884906, E-mail: gerber@physik.uni-wuerzburg.de)
[3] Arthur Amos Noyes Laboratory of Chemical Physics, California Institute of Technology, Pasadena, California 91125, USA

Abstract. Femtosecond time-resolved photoion and photoelectron spectroscopy were employed to study the transition state dynamics of *cis*-stilbene in a molecular beam experiment. Two long-lived photoproducts were found with excitation of 267 nm radiation.

PACS: 82.30.Qt; 82.40.Js; 82.50.Fv; 82.80.Ms; 82.80.Pv

With the exceptional time resolution of femtosecond lasers, a new era in studying atomic, molecular and condensed matter processes has begun [1, 2]. For the first time it has become possible to directly observe primary photophysical, photochemical and photobiological processes in real time. A variety of different detection schemes have been successfully implemented for this purpose, such as ion mass spectrometry [1, 3] and photoelectron spectroscopy [4–6], transient absorption spectroscopy [7], laser-induced fluorescence (LIF) [8], and electron [9, 10] and X-ray scattering [11, 12].

Ion mass spectrometry in combination with femtosecond pump–probe and molecular beam techniques has been applied successfully to investigate the photodissociation dynamics of large molecules [1, 13]. The energy resolved detection of the corresponding photoelectrons has proven to be a powerful tool in studying primary processes in small molecules with high temporal and spatial resolution [6]. Today, molecular dynamics in neutral intermediate states can be mapped along the reaction coordinate without being limited to only a small fraction of internuclear distances or bond angles. Several groups have employed femtosecond time-resolved photoelectron spectroscopy studies on large molecules in the gas phase [14–16].

In this paper, we use ion mass spectrometry as well as photoelectron spectroscopy in combination with pump–probe and molecular beam techniques to study the femtosecond transition state dynamics of stilbene. This molecule is an extensively studied prototype system, experimentally ([17–22] and references therein) as well as theoretically [23]. A variety of different techniques to study the geometrical *cis–trans*

and the *trans–cis* isomerization process, as well as electronic rearrangement to yield 4a,4b-dihydrophenanthrene (DHP), have been used in liquid phase experiments. However, only recently has information become available about those processes for the isolated molecule in the gas phase [24–27].

For *cis*-stilbene, Greene and Farrow [25] were the first to measure the initial decay in the gas phase at room temperature with sub-picosecond laser pulses, and they reported a lifetime for the electronically excited molecule of 320 fs when excited with 312 nm. For 285 nm excitation wavelengths, Pedersen et al. [27] reported a lifetime of 360 fs. Additionally, they observed a coherent wavepacket motion, which was attributed to a phenyl torsional motion of the molecule while undergoing isomerization. Similar results were obtained by Szarka et al. [28] in solution while observing solvent-dependent wavepacket dynamics.

Here we report the observation of the ultrafast dynamics of the transition state (TS) in the isomerization reaction of *cis*-stilbene under collisionless conditions. The excitation scheme of the experiment is depicted in Fig. 1 and shows the S_0 and the S_1 potential energy surfaces (PES) for the *cis–trans* isomerization coordinate θ (adapted from [29]). As the ionic potential (IP) is known only for $\theta = 0°$ and $\theta = 180°$ and these values only differ by ≈ 150 meV, the IP is approximated to be constant for this reaction coordinate. In order to study the excited state dynamics of *cis*-stilbene, a 267 nm pump laser pulse excites the molecule from the S_0 ground-state to the S_1 excited-state potential energy surface. The excitation wavelength matches the broad absorption band of the ground-state *cis*-stilbene [29, 30]. The temporal evolution of the excited molecular system is then probed by a time-delayed 400 nm laser pulse by ionizing the system.

1 Experimental setup

The femtosecond laser pulses are provided by a home-built Ti:Sapphire oscillator with a chirped pulse amplification (CPA) system. Output pulses of 800 nm (90 fs, 1 mJ, 1 kHz) are frequency-doubled to yield pulses of 400 nm by second harmonic generation (SHG) in a 100 μm BBO crystal. By
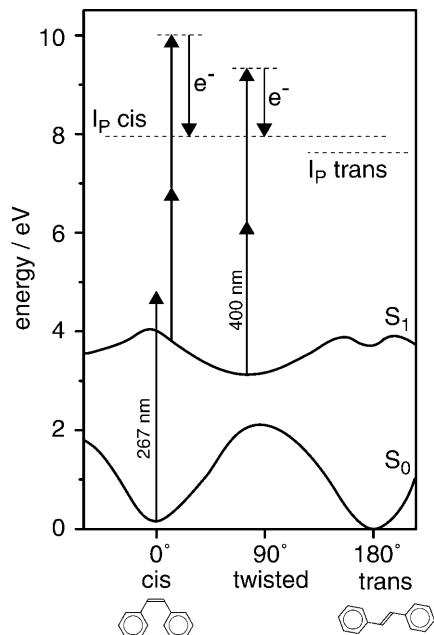
---

*Corresponding author.

Fig. 1. Excitation scheme. The ground state (S_0) and excited state (S_1) potential energy surfaces (PES) are shown along the *cis–trans* isomerization angle θ (adapted from [29]). The ionic PES are not yet known. Therefore only the thresholds for ionization are depicted (*dotted lines*)

sum frequency mixing of the fundamental and the second harmonic in a second BBO crystal (100 μm), the third harmonic is generated yielding 267 nm pulses. In a Mach–Zehnder interferometer the 267 nm pulses are separated from the 400 nm pulses with a dichroic beam splitter and time delayed by a computer-controlled translation stage. The two beams are finally recombined collinearly and focused with a 300 mm quartz lens into the vacuum chamber. Both beams can be attenuated separately to adjust the intensity of the pump and probe lasers.

To generate a molecular beam of *cis*-stilbene, we employ the seeded-beam technique. *Cis*-stilbene vapor from a liquid reservoir at room temperature is coexpanded with the inert carrier gas helium (≈ 1.5 bar) through a nozzle of ≈ 200 μm diameter. The molecular beam is skimmed and directed through the pole-pieces of a magnetic bottle electron spectrometer [31] (MBES, Applied Laser Technology), where it intersects the laser beam perpendicularly (see Fig. 2). The time of flight (TOF) distribution of the photoelectrons is recorded with the MBES employing a 1 GHz, 2 gigasample digital oscilloscope, and the spectra are averaged over several thousands of laser shots. The energy resolution is 30 meV for electrons with a kinetic energy of 0.7 to 1.0 eV. A small extraction voltage of 1.5 V is applied to enhance the detection probability of photoelectrons of almost-zero kinetic energy. The TOF photoelectron spectra are calibrated using the well-known electron spectra of atomic xenon and krypton.

In addition a linear TOF mass spectrometer is used to detect the corresponding ions. This enables us to compare the excitation condition in the photoelectron experiment with that in the multiphoton ionization case of *cis*-stilbene dynamics.

The *cis*-stilbene (Sigma Aldrich, purity $\approx 97\%$) was used without further purification. According to [25] an impurity of *trans*-stilbene would only lead to a long lifetime component in the pump–probe transients, which we did not observe.
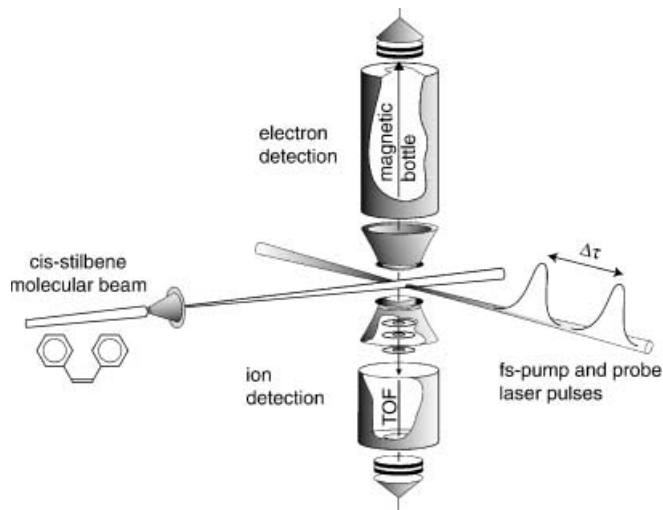

Fig. 2. Experimental setup. A molecular beam of *cis*-stilbene intersects (perpendicularly) the laser beam in a high vacuum chamber. The formed ions are detected by a linear time-of-flight (TOF) mass spectrometer, while the corresponding photoelectrons are recorded with a magnetic bottle electron spectrometer

2 Experiment and discussion

2.1 Ion spectroscopy

Figure 3a shows a mass spectrum of *cis*-stilbene obtained with the probe laser pulse alone (400 nm), with a pulse energy of $E \approx 10$ μJ. A clear peak appears at a mass of 180 amu, which can be assigned to the mass peak of the parent ion. Additionally, a variety of fragment ions are observed, which result from the subsequent loss of C_xH_y groups from the parent molecule. Note, that due to the limited resolution of the spectrometer, the loss of H atoms cannot be resolved, and therefore the observed ion signal is an
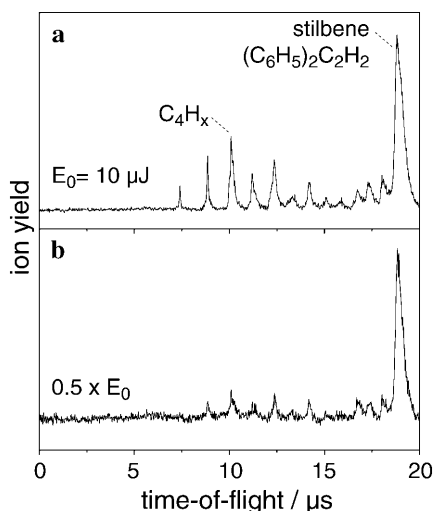

Fig. 3a,b. Mass spectra. **a** The interaction of the stilbene molecule with femtosecond laser pulses at 400 nm leads to ionization and fragmentation of the parent molecule. **b** By lowering the laser pulse energy, the fragmentation process can be significantly reduced. Note that the broad peaks result from a successive loss of H atoms, which cannot be resolved with the mass spectrometer used in this experiment

integral measure of the number of photoproducts ($C_{14}H_x$, $x = 12 \ldots 8$ and C_4H_x, $x = 4 \ldots 0$). Reducing the laser pulse energy to $E \approx 5\,\mu J$, the fragments nearly disappear and only the stilbene parent ion is produced (Fig. 3b). This behavior is in agreement with femtosecond experiments on the photodissociation of large organometallic molecules, where the relative photoproduct yields strongly depend on the applied laser pulse intensity as well as on the pulse duration [13]. For decreasing pulse energy as well as for decreasing pulse duration, the yield of the smaller fragments is reduced.

For an investigation of the TS dynamics of *cis*-stilbene after femtosecond excitation, a pump–probe experiment was performed with properly attenuated laser pulse intensities, such that neither pump nor probe produced any ion signal. The dynamics initiated by a 267 nm pump laser pulse was probed with a time-delayed 400 nm probe laser pulse. The transient ion yield of the parent molecule *cis*-stilbene and that of the fragment C_4H_x were recorded (Fig. 4).

The parent and the fragment transients were fitted with exponential functions. In order to take into account the temporal resolution of the experiment, the molecular response was convoluted with a Gaussian (FWHM = 400 fs). For the parent molecule, a decay time of $\tau_{\text{decay}} = 320 \pm 10\,\text{fs}$ was found, giving a lifetime of the transition state consistent with the range observed in earlier experiments [25, 27]. The C_4H_x transient showed a decay time of the order of 1 ps. The ion signal seemed to reach a constant level for longer delay times, indicating an additional rising component. Due to the poor signal-to-noise ratio, we cannot assign a time constant for this rising component. However, the existence of an additional component is consistent with a sequential dissociation model where C_4H_x is due to a dissociation of a larger photoproduct. A detailed investigation of the photodissociation mechanisms taking into account all the observable photoproducts with a better time resolution is currently underway.
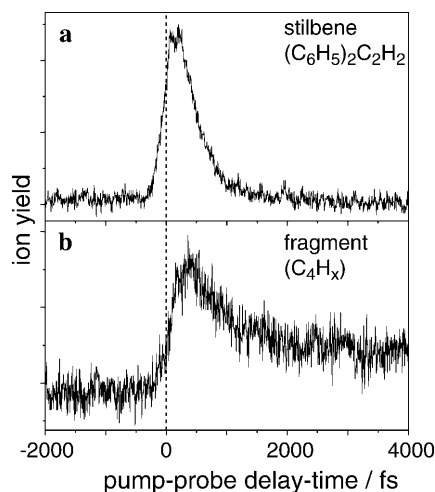
2.2 Photoelectron spectroscopy

As well as ion mass spectrometry, energy-resolved photoelectron spectroscopy was employed. Figure 5a and b show the photoelectron spectra obtained with the pump laser (267 nm) and the probe laser (400 nm). Both spectra show a broad energy distribution. By calibrating the electron spectrometer, the kinetic energies of the observed photoelectrons were determined to range from 0 eV to almost 1.5 eV. The *cis*-stilbene molecule is ionized either by a three-photon excitation with 400 nm or by a two-photon excitation with 267 nm radiation (Fig. 1). Although the total excitation energy is the same in both measurements, the corresponding spectra look quite different. The spectrum shown in Fig. 5c was recorded employing pump and probe laser pulses at a delay time of 5 ps. It is essentially the sum of the spectra obtained with the pump and probe lasers individually. The coarse structure in the photoelectron spectra are not assigned yet, because the involved PES are not yet known accurately enough.

We also measured the photoelectron spectra, using the same wavelengths as for the mass spectra. The shape of the spectra does not change for the two pulse energies E_0 and $0.5 \cdot E_0$. This is clear evidence that all the detected photoelectrons have their origin in the photoionization process of the parent molecule *cis*-stilbene.

In order to monitor the dynamics of the wave packet motion on the excited state PES S_1 started by the 267 nm pump laser, two segments of the TOF electron spectrum (Fig. 5c, gray blocks) were integrated and recorded as a function of the delay time between the pump and probe laser pulses. Those windows were selected such that one measures two clearly separated kinetic energies, one at $0.9\,\mu s$ (1.1 eV) and the second at $1.4\,\mu s$ (0.25 eV). Figure 6 shows the transient photoelectron signals at these two different kinetic energies. The transients are normalized, and the time-independent con-
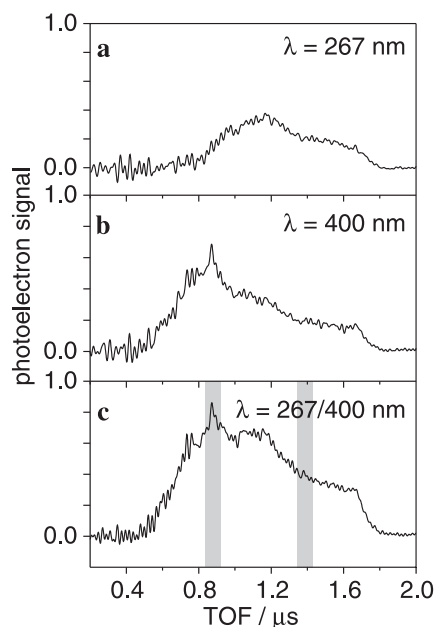

Fig. 4a,b. Ion pump–probe spectra. The 267 nm pump/400 nm probe transients are plotted **a** for the stilbene molecule and **b** for the photofragment C_4H_x, $x = 4 \ldots 0$ (see Fig. 3). Whereas the parent molecule shows a single exponential decay, the fragment transient exhibits a decay as well as a rise time component, resulting in a time-independent plateau at positive delay times

Fig. 5a–c. Photoelectron spectra. The photoelectron yield was recorded applying **a** the pump laser at 267 nm and **b** the probe laser at 400 nm. **c** The signal of both lasers at a delay time of 5 ps. *Gray blocks*: integration windows in the pump–probe experiment (see text)
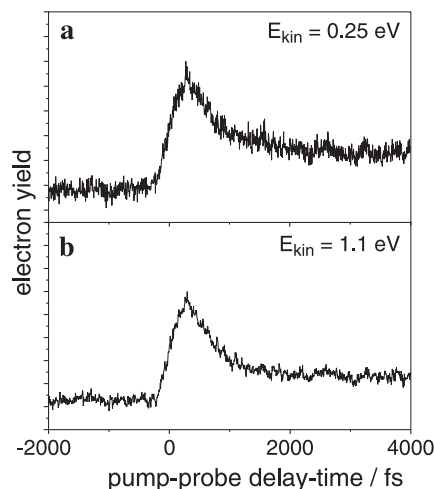
Fig. 6a,b. Pump–probe photoelectron spectra. The 267 nm pump/400 nm probe transients are plotted for the photoelectrons of **a** 0.25 eV and **b** 1.1 eV (see Fig. 5). Both transients show an exponential decay component with a similar time constant going down to significantly different levels at positive delay times

tribution for negative delay times, where the 400 nm laser interacts first, was set to zero. The transients were fitted to an exponential function convoluted with a Gaussian (FWHM = 400 fs). The decay time constants are similar in both transients ($\tau_{decay} \approx 450$ fs), whereas the levels of the constant plateaus at positive delay times are significantly different. This indicates two different rising components. By including these time dependencies into the molecular response function, the decay and rise time constants would be strongly correlated for the given transients. Therefore we cannot give accurate time constants. However, the existence of these plateaus is an indication that long-lived photoproducts are formed after the initial excitation to the transition state of *cis*-stilbene.

In future experiments the complete TOF electron spectra will be recorded as a function of the delay time. Such experiments together with theoretical calculations of the involved PES would give much more insight into the transition state dynamics and would allow a detailed interpretation of the observed dynamics of *cis*-stilbene and its isomerization into the *trans* species as well as into the DHP species.

3 Conclusion

We applied femtosecond time-resolved photoelectron and ion spectroscopy to study a configurational rearrangement in a large organic molecule in real time. The transition state dynamics of gas phase *cis*-stilbene indicates that long-lived photoproducts are prepared with 267 nm excitation.

References

1. A.H. Zewail: *Femtochemistry* Vols. I and II (World Scientific, Singapore 1994)
2. J. Manz, L. Wöste: *Femtosecond Chemistry* Vols. I and II (VCH, Weinheim 1995)
3. T. Baumert, B. Bühler, R. Thalweiser, G. Gerber: Phys. Rev. Lett. **64**, 733 (1990)
4. T. Baumert, R. Thalweiser, G. Gerber: Chem. Phys. Lett. **209**, 29 (1993)
5. D.R. Cyr, C.C. Hayden: J. Chem. Phys. **104**, 771 (1996)
6. A. Assion, M. Geisler, J. Helbing, V. Seyfried, T. Baumert: Phys. Rev. A **54**, R4605 (1996)
7. G.R. Fleming: *Chemical Applications of Ultrafast Spectroscopy* (Oxford University Press, New York 1986)
8. M.J. Rosker, M. Dantus, A.H. Zewail: J. Chem. Phys. **89**, 6113 (1988)
9. J.C. Williamson, J. Cao, H. Ihee, H. Frey, A.H. Zewail: Nature (London) **386**, 159 (1997)
10. H. Ihee, J. Cao, A.H. Zewail: Chem. Phys. Lett. **281**, 10 (1997)
11. F. Raksi, K.R. Wilson, Z. Jiang, A. Ikhlef, C.Y. Côté, J.C. Kieffer: J. Chem. Phys. **104**, 6066 (1996)
12. C. Rose-Petruck, R. Jimenez, T. Guo, A. Cavalleri, C.W. Siders, F. Raksi, J.A. Squier, B.C. Walker, K.R. Wilson, C.P.J. Barty: Nature (London) **398**, 310 (1999)
13. L. Banares, T. Baumert, M. Bergt, B. Kiefer, G. Gerber: J. Chem. Phys **108**, 5799 (1998)
14. B.J. Greenblatt, M.T. Zanni, D.M. Neumark: Chem. Phys. Lett: **258**, 523 (1996)
15. V. Stert, W. Radloff, C.P. Schulz, I.V. Hertel: Euro. Phys. J. D **5**, 97 (1999)
16. V. Blanchet, M.Z. Zgierski, T. Seideman, A. Stolow: Nature (London) **401**, 52 (1999)
17. J. Saltiel, Y.-P. Sun: *Photochromism – Molecules and Systems*, ed. by H. Dürr, H. Bouas-Laurent (Elsevier, Amsterdam 1990) p 64
18. D.H. Waldeck: Chem. Rev. **91**, 415 (1991)
19. R.J. Sension, S.T. Repinec, A.Z. Szarka, R.M. Hochstrasser: J. Chem. Phys. **98**, 6291 (1993)
20. L. Nikowa, D. Schwarzer, J. Troe, J. Schroeder: J. Chem. Phys. **97**, 4827 (1992)
21. D.C. Todd, G.R. Fleming: J. Chem. Phys. **98**, 269 (1993)
22. A. Meyer, J. Schroeder, J. Troe: J. Phys. Chem. A **103**, 10528 (1999)
23. M.J. Bearpark, F. Bernardi, S. Clifford, M. Olivucci, M.A. Robb, T. Vreven: Phys. Chem. A **101**, 3841 (1997)
24. J.A. Syage, W.R. Lambert, P.M. Felker, A.H. Zewail, R.M. Hochstrasser: Chem. Phys. Lett. **88**, 266 (1982)
25. B.I. Greene, R.C. Farrow: J. Chem. Phys. **78**, 3336 (1983)
26. J.H. Frederick, Y. Fujiwara, J.H. Penn, K. Yoshihara, H. Petek: J. Phys. Chem. **95**, 2845 (1991)
27. S. Pedersen, Bañares, A.H. Zewail: J. Chem. Phys. **97**, 8801 (1992)
28. A.Z. Szarka, N. Pugliano, D.K. Palit, R.M. Hochstrasser: Chem. Phys. Lett. **240**, 25 (1995)
29. S. Abrash, S. Repinec, R.M. Hochstrasser: J. Chem. Phys. **93**, 1041 (1990)
30. J. Saltiel, A.S. Waller, D.F. Sears, Jr.: J. Photochem. Photobiol. A **65**, 29 (1992)
31. P. Kruit, F.H. Read: J. Phys. E **16**, 313 (1983)